

Supporting Information

Non-Nitric oxide Based Metallovasodilators: Synthesis, Reactivity and Biological Studies

Denise S. Sá^{a,b}, Carlos D. S. Silva^{a,b}, André F. Fernandes^b, Paula P. C. Costa^c,
Manassés C. Fonteles^c, Nilberto R. F. Nascimento^c, Luiz G. F. Lopes^b and
Eduardo H. S. Sousa^b *

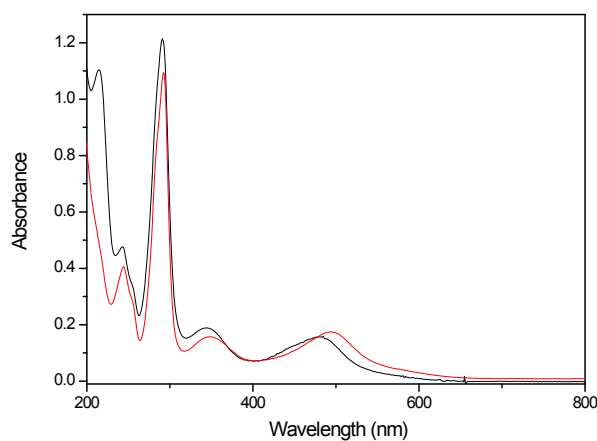


Figure S1. Electronic absorption spectra of FOR007 (black) and FOR000 (red) in acetonitrile.

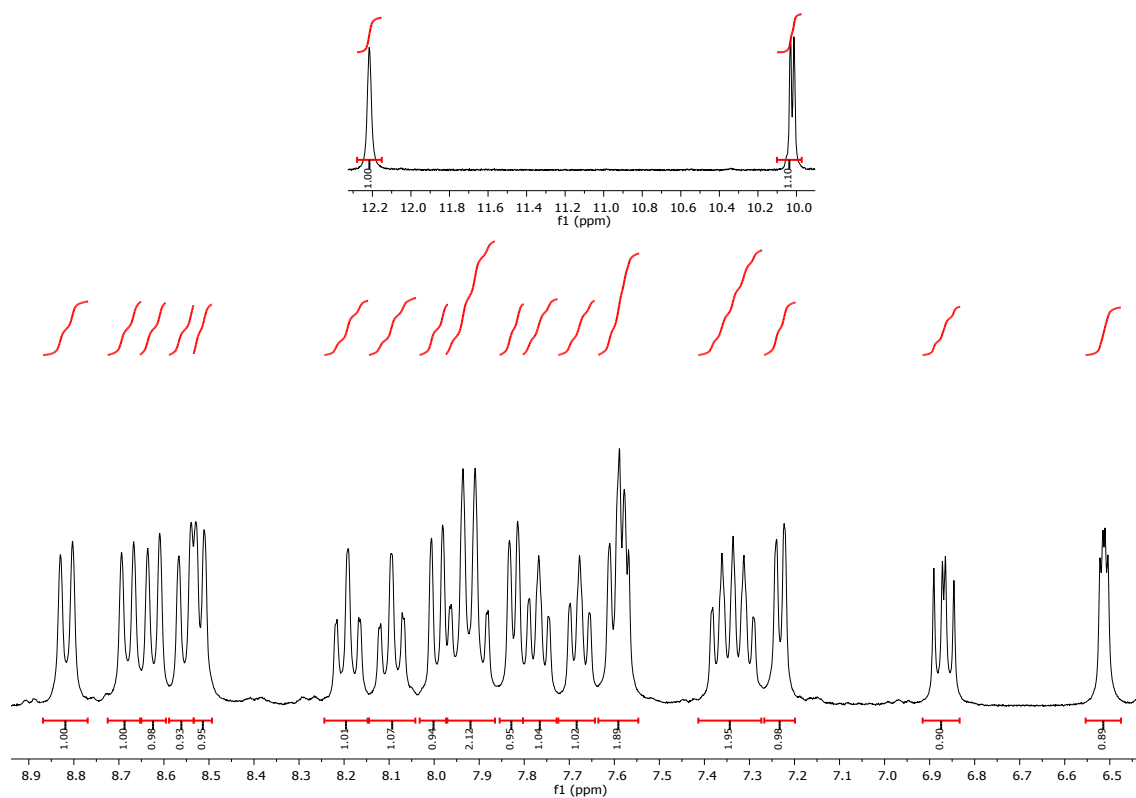


Figure S2. ^1H NMR spectrum of cis- $[\text{RuCl}(\text{ain})(\text{bpy})_2]\text{PF}_6$ (FOR007) in deuterated DMSO.

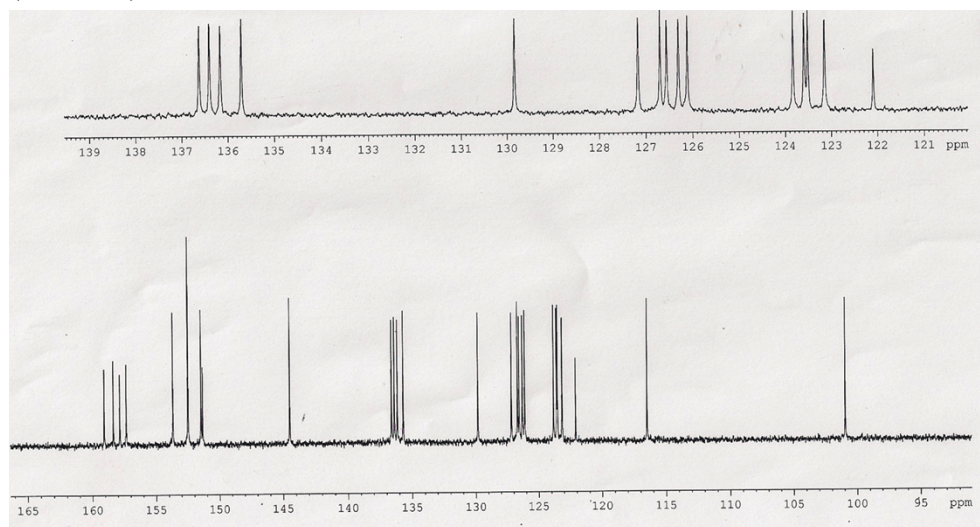
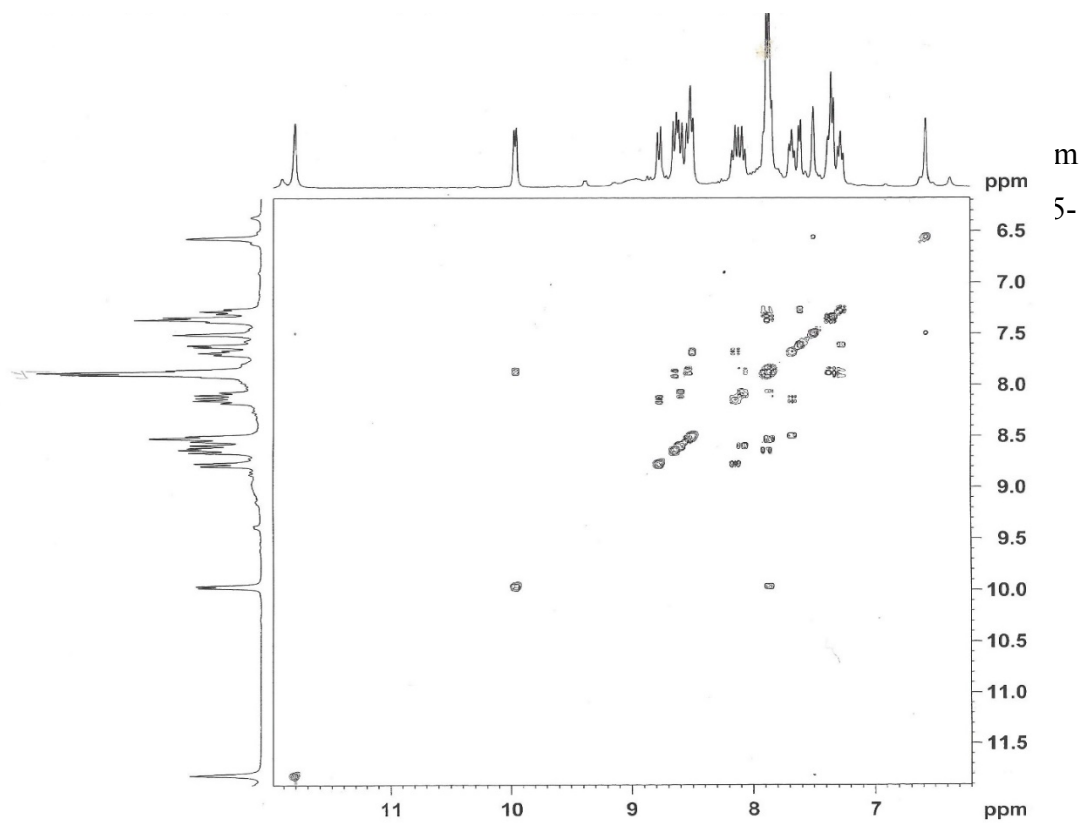


Figure S3. ^{13}C NMR spectrum of cis- $[\text{RuCl}(\text{ain})(\text{bpy})_2]\text{PF}_6$ (FOR007) in deuterated DMSO.

deuterated DMSO (bottom: full spectrum, top: expansion of region).



$[\text{Ru}(\text{bpy})_3]^{2+}\text{PF}_6^-$ (FOR005) in deuterated DMSO.

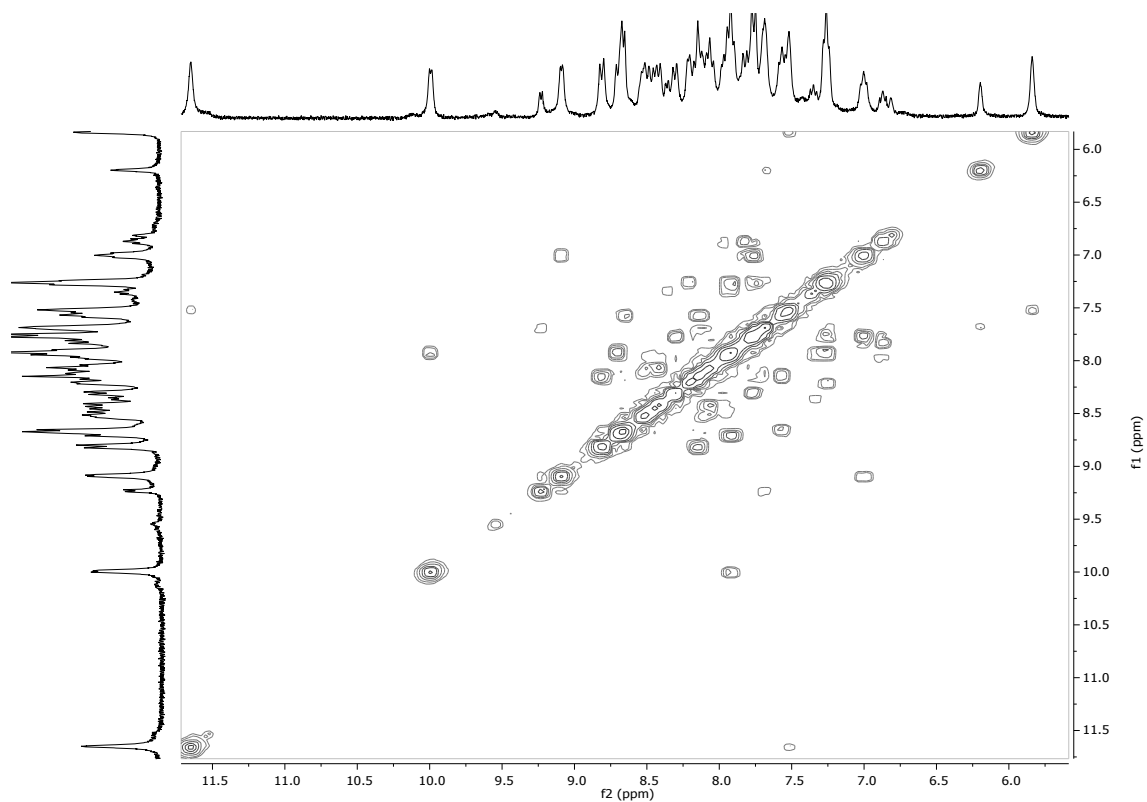


Figure S4-B. COSY spectrum of $\text{cis-}[\text{RuCl}(4\text{-ain})(\text{bpy})_2]\text{PF}_6$ (FOR004) in deuterated DMSO.

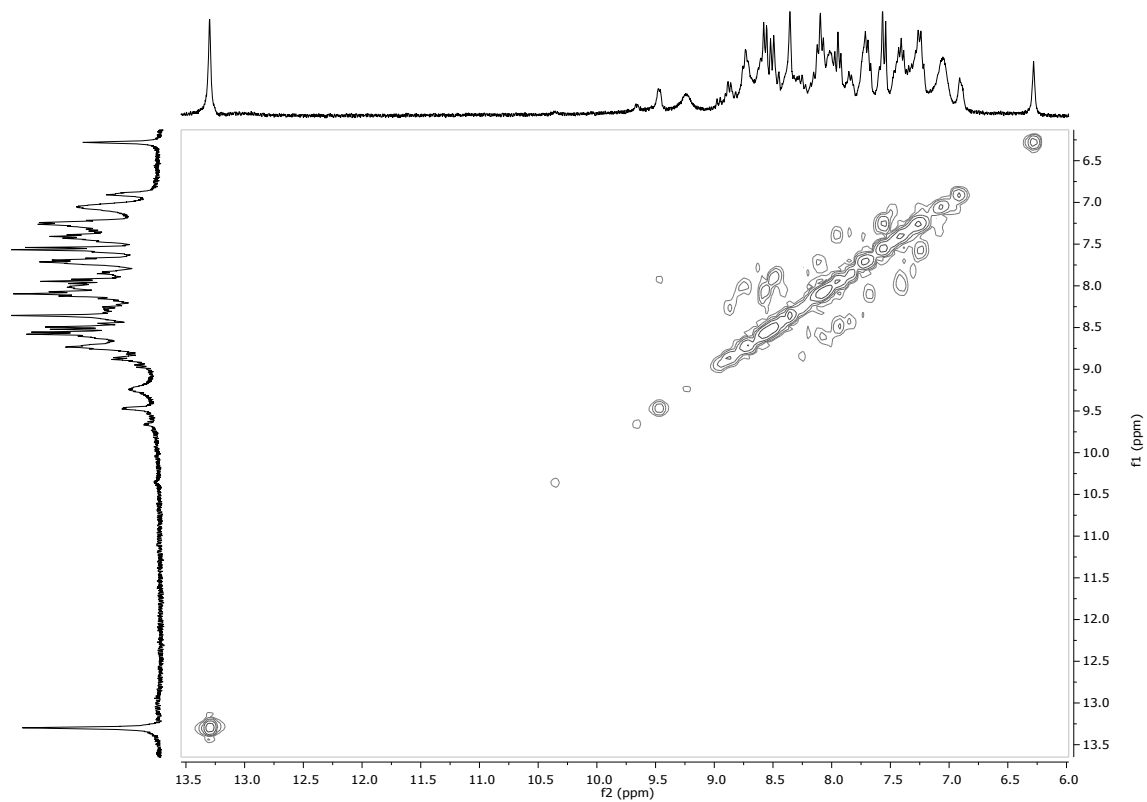


Figure S4-C. COSY spectrum of $\text{cis-}[\text{RuCl}(\text{bzim})(\text{bpy})_2]\text{PF}_6$ (FOR003) in deuterated DMSO.

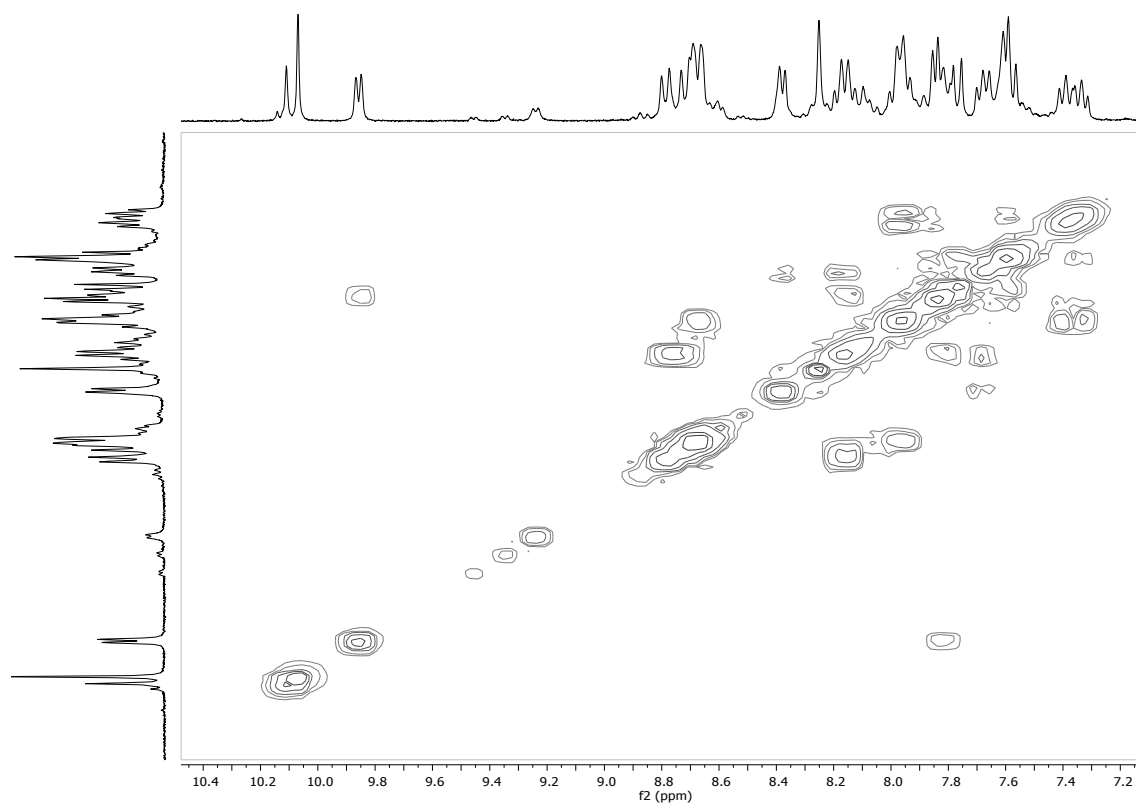


Figure S4-D. COSY spectrum of $\text{cis-}[\text{RuCl}(\text{COH-indz})(\text{bpy})_2]\text{PF}_6$ (FOR002A) in deuterated DMSO.

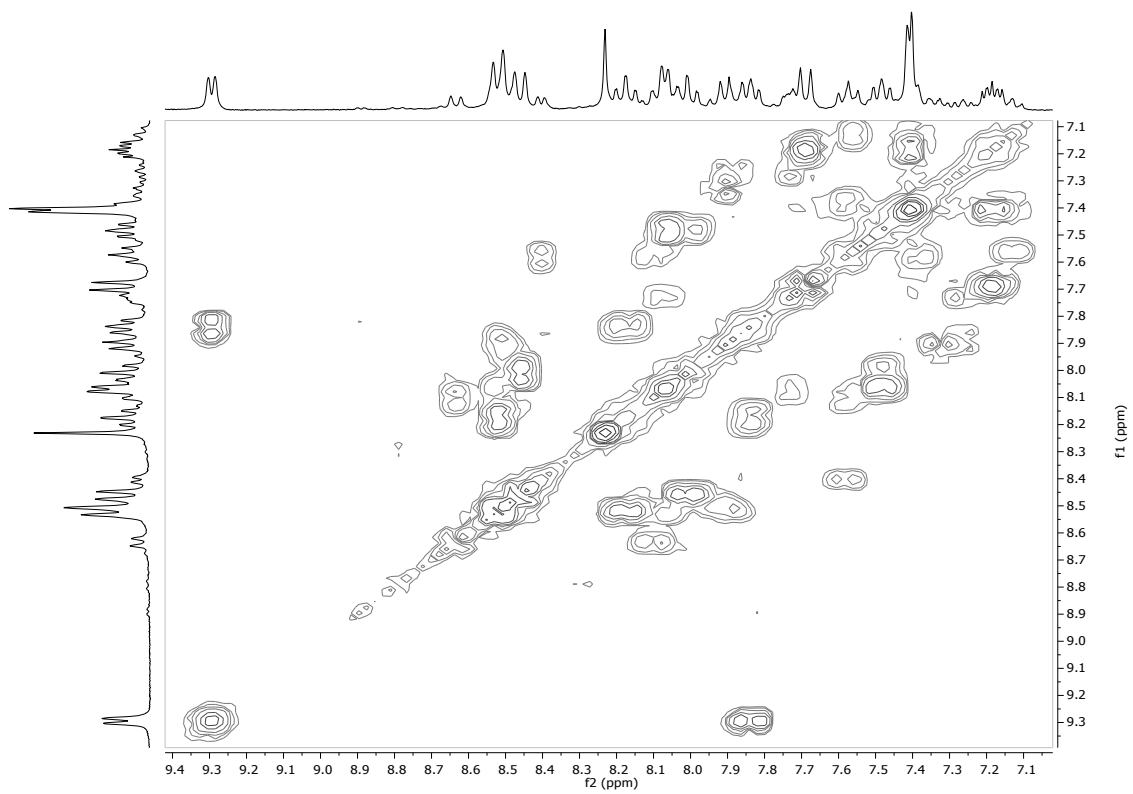


Figure S4-E. COSY spectrum of $\text{cis-}[\text{RuCl}(\text{indz})(\text{bpy})_2]\text{PF}_6$ (FOR002) in CD_3OD .

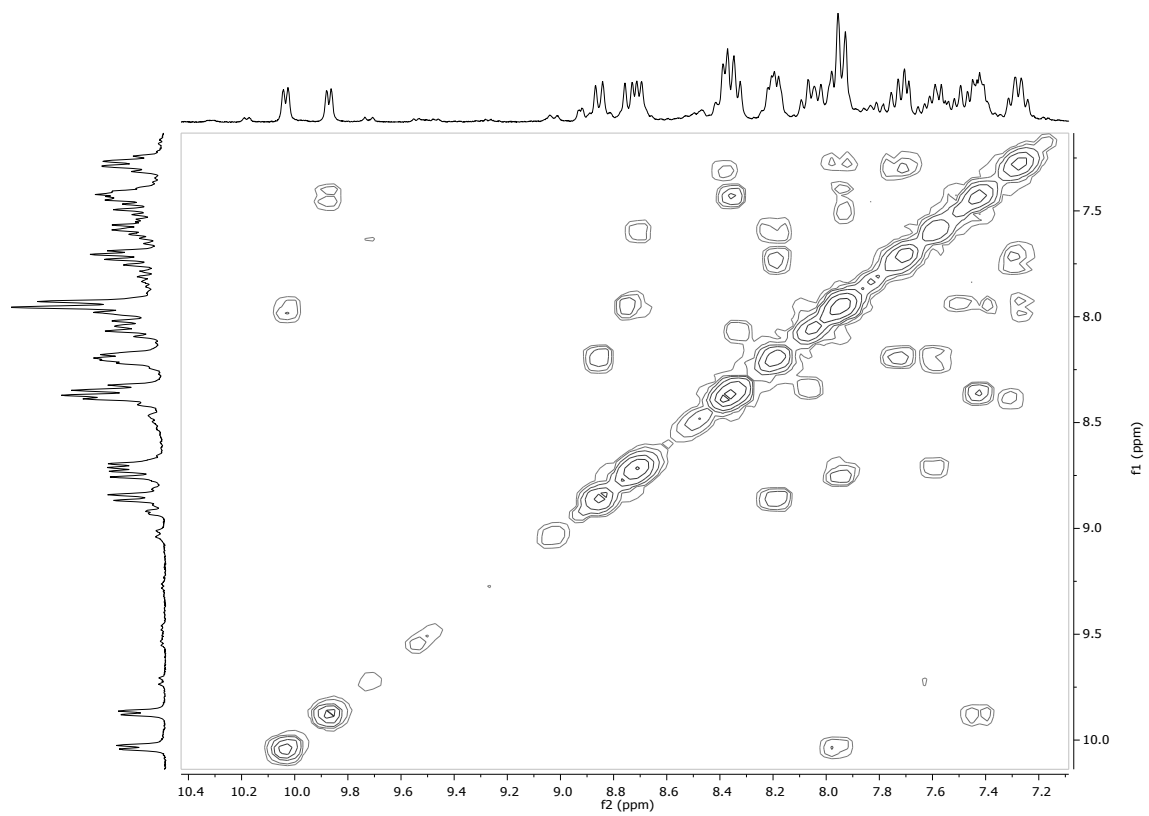


Figura S4-F. COSY spectrum of $\text{cis-}[\text{RuCl}(\text{qui})(\text{bpy})_2]\text{PF}_6$ (FOR001) in deuterated DMSO.

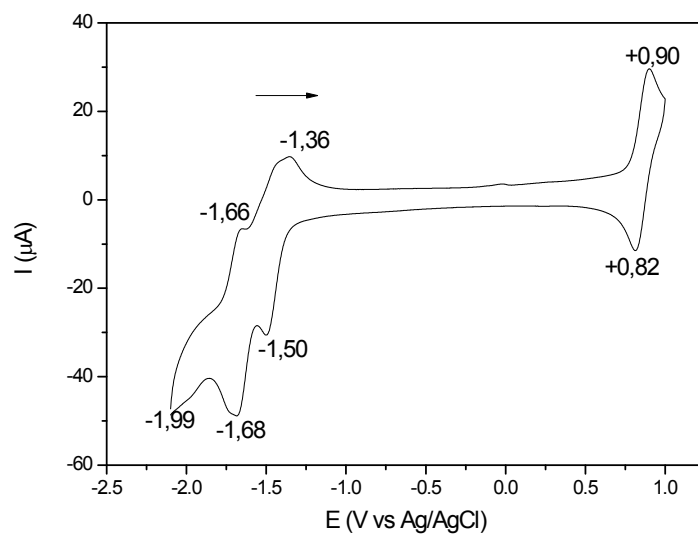


Figure S5-A. Cyclic voltammogram for complexes FOR002 in acetonitrile /tetrabutylammonium perchlorate (PTBA), 0.1 mol.L⁻¹. Rate scan: 100 mV.s⁻¹.

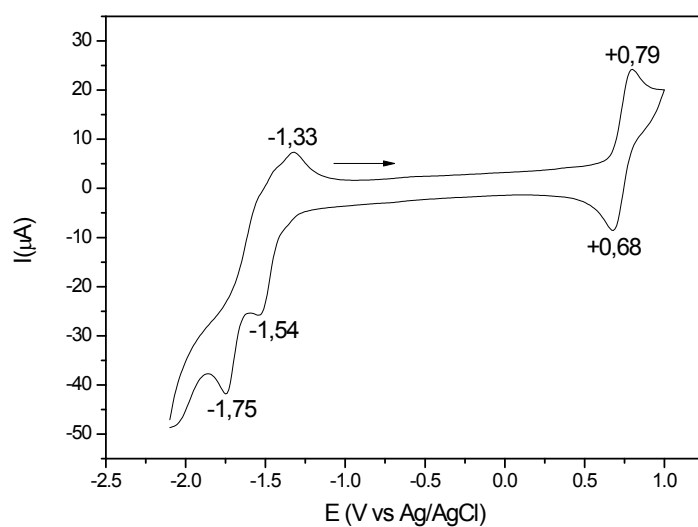


Figure S5-B. Cyclic voltammogram for complexes FOR005 in acetonitrile /tetrabutylammonium perchlorate (PTBA), 0.1 mol.L⁻¹. Rate scan: 100 mV.s⁻¹.

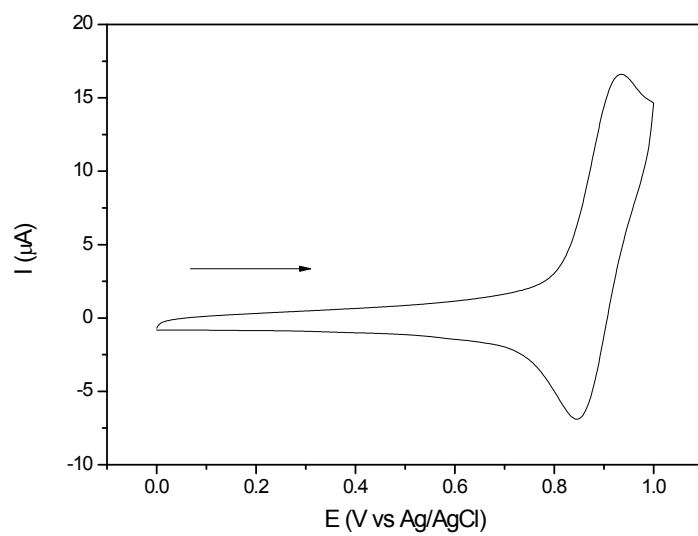
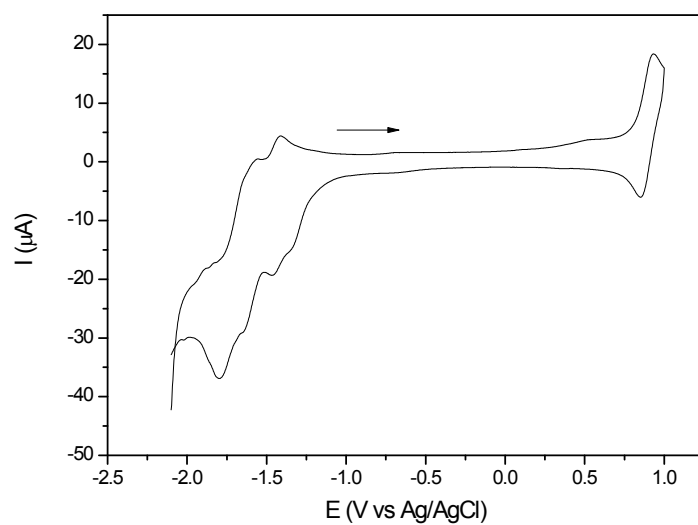


Figure S5-C. Cyclic voltammogram for complexes FOR002A in acetonitrile /tetrabutylammonium perchlorate (PTBA), 0.1 mol.L^{-1} full window (top) or positive windows scan (bottom). Rate scan: 100 mV.s^{-1} .

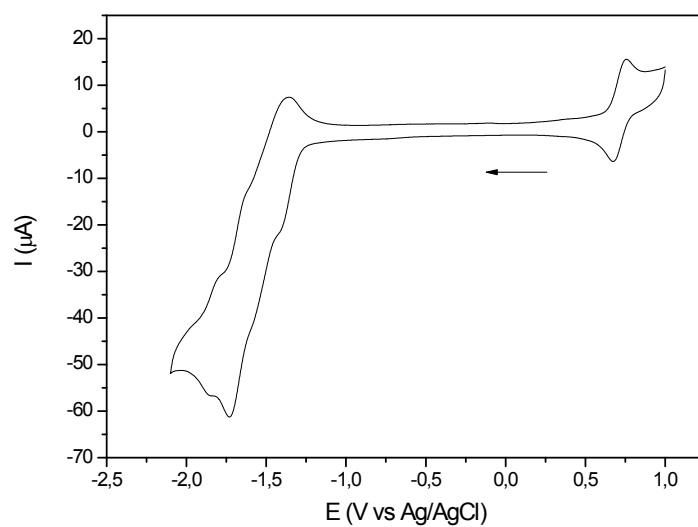


Figure S5-D. Cyclic voltammogram for complexes FOR003 in acetonitrile /tetrabutylammonium perchlorate (PTBA), 0.1 mol.L⁻¹. Rate scan: 100 mV.s⁻¹.

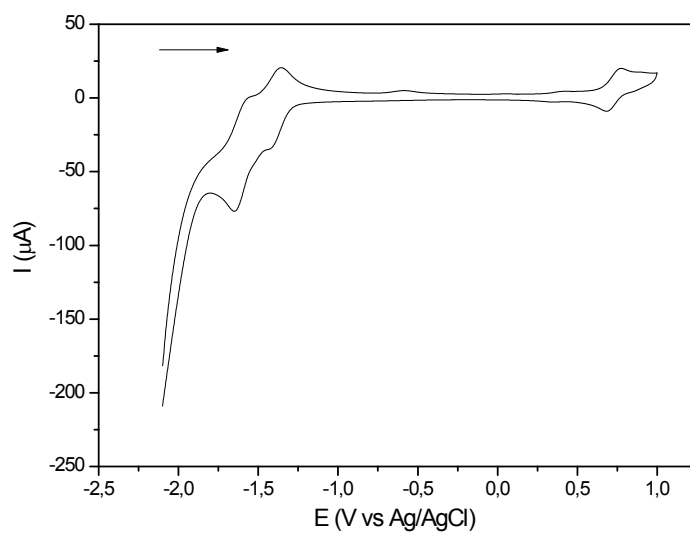


Figure S5-E. Cyclic voltammogram for complexes FOR004 in acetonitrile /tetrabutylammonium perchlorate (PTBA), 0.1 mol.L⁻¹. Rate scan: 100 mV.s⁻¹.

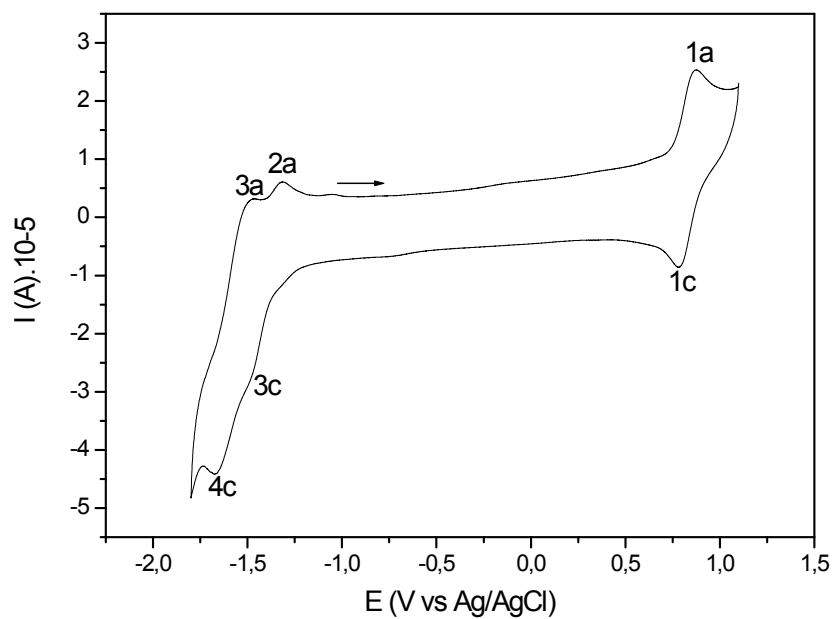


Figure S5-F. Cyclic voltammogram for complexes FOR001 in acetonitrile /tetrabutylammonium perchlorate (PTBA), 0.1 mol.L⁻¹. Rate scan: 100 mV.s⁻¹.

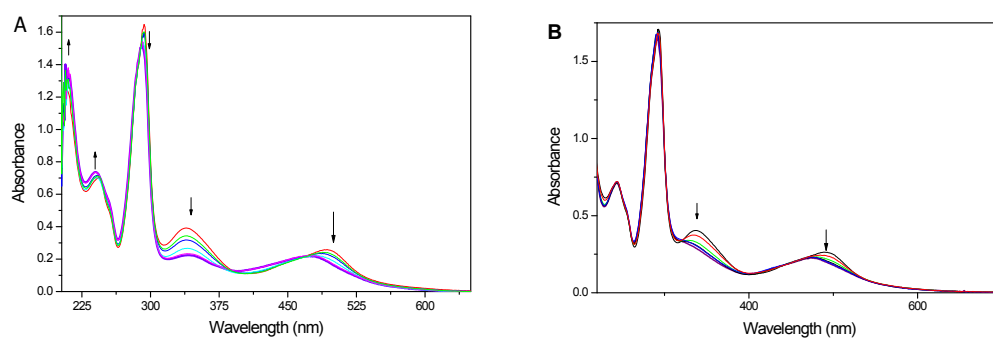


Figure S6-A. Electronic absorption spectra of FOR002 in (A) acetonitrile and (B) methanol, during successive light irradiation at 300 nm for ca. 22 minutes.

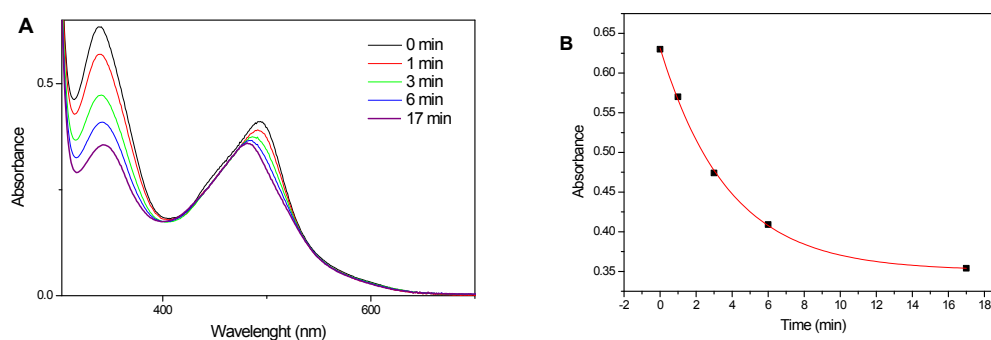
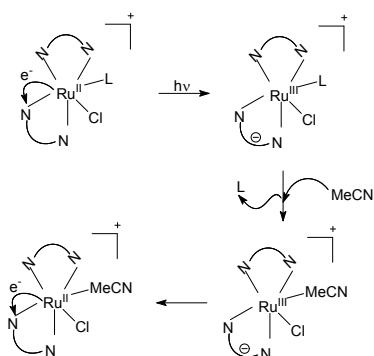


Figure S6-B. Electronic absorption spectra of FOR002 in acetonitrile during successive light irradiation at 420 nm (A) and kinetic curve for this process as measured at 334 nm (B).

Table S1. Electronic spectroscopy data for *cis*-[RuCl(L)(bpy)₂]⁺ upon light irradiation at 300 nm in acetonitrile.

	Dark(nm)	Light(nm)
FOR002	493	480
	337	343

FOR007	492	480
	351	345
FOR005	513	480
	351	345
FOR001	492	480
	377	345
FOR004	497	480
	355	345



Scheme S1. Proposed mechanism of photorelease for the $[\text{Ru}(\text{bpy})_2\text{LCl}]^{2+}$ complex

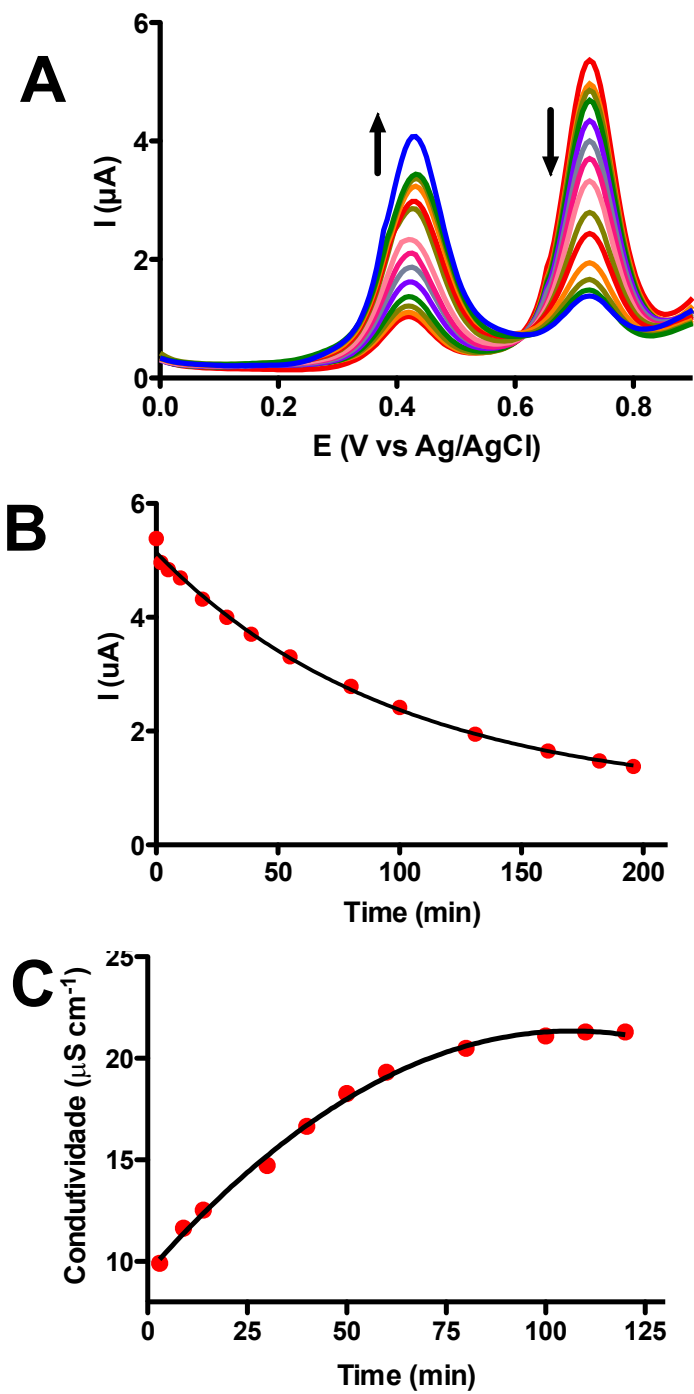


Figure S7- Reactivity of FOR007 (0.8 mM) in phosphate buffer solution pH 7.4 (10% DMF), anodic curve at sweep rate of 25 mV s^{-1} (A). Kinetic plot for peak current at 0.74V (B). Conductivity measured overtime for FOR007 dissolved in water (10% DMF) (C).

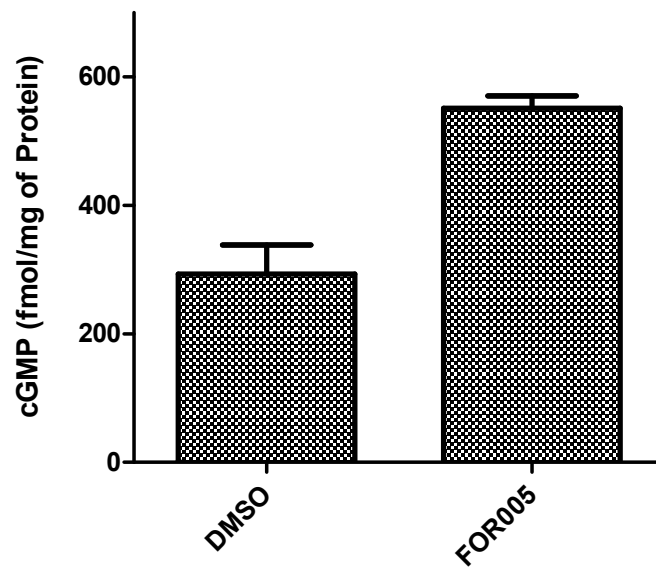


Figure S8. Measurement of total cGMP production (cGMP ELISA kit) in vascular tissue treated with dms0 (control) and FOR005 (n = 6, ANOVA followed by Bonferroni test).

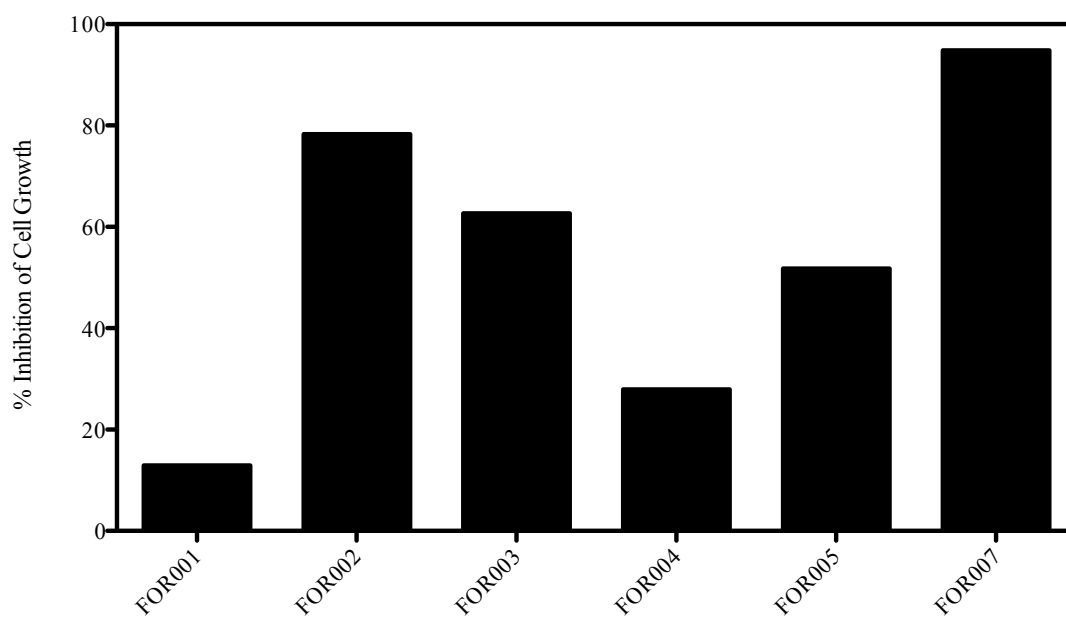


Figure S9. Cell growth inhibition for HCT-116 cancer cells (35 μM of metal compound).

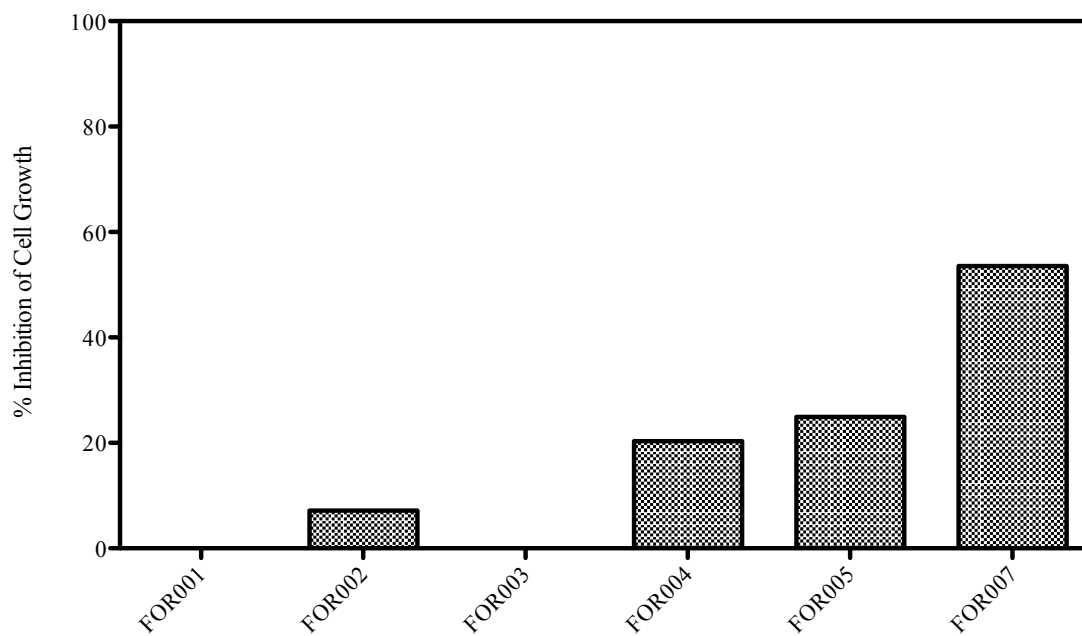


Figure S10. Cell growth inhibition for ovc8 cancer cells (35 μM of metal compound).

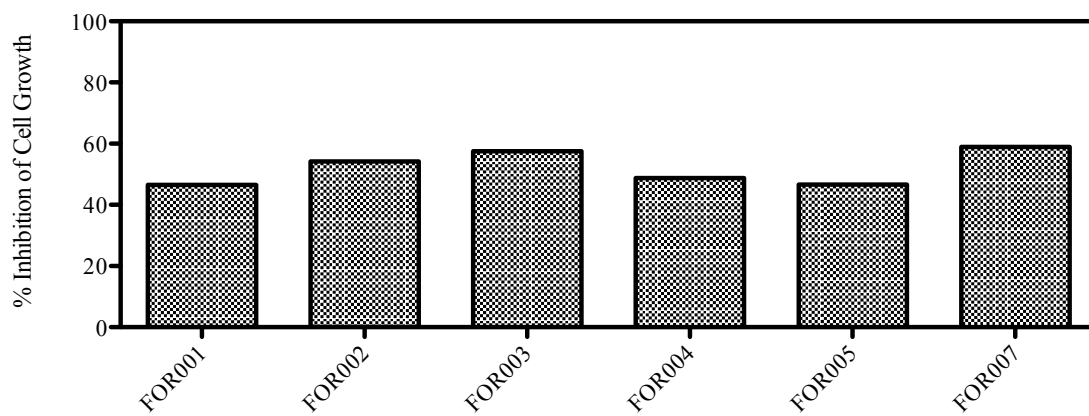


Figure S11. Cell growth inhibition for SF-295 cancer cells (35 μM of metal compound).

Table S2. Cytotoxicity IC_{50} values measured for two selected complexes

	IC_{50} (μM)			
	HL-60	Ovcar-8	SF-295	HCT-116
FOR002	5.8	>35	16.0	9.7
FOR007	15.0	>35	>35	13.5

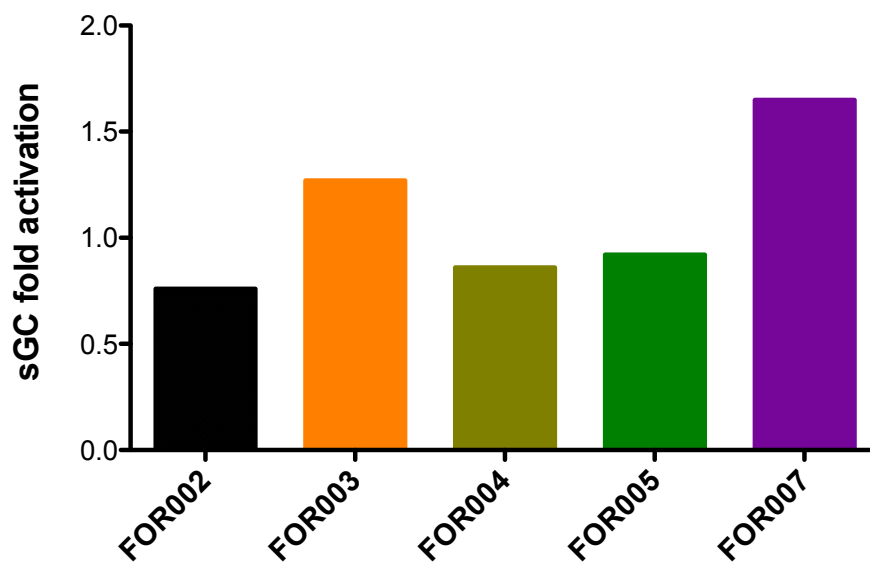


Figure S12. Assay of sGC activation using FOR002, FOR003, FOR004, FOR005, FOR007 complexes at 100 μ M, without any stimulation with NO donors, at 37 $^{\circ}$ C.